# Copper Fixation to Guaiacyl Lignin Units by Nitrogen Donor Ligands

Bojan Kozlevčar, Polonca Bašković, Aleksej Arko, Amalija Golobič, Nives Kitanovski, and Primož Šegedin

Faculty of Chemistry and Chemical Technology, University of Ljubljana, 1001 Ljubljana, Slovenia

Reprint requests to Bojan Kozlevčar. E-mail: bojan.kozlevcar@fkkt.uni-lj.si

*Z. Naturforsch.* **2008**, *63b,* 481 – 488; received January 7, 2008

Several new copper(II) complexes with guaiacyl lignin models vanillin (HL1) $[Cu(L1)_2(nia)_2]$ (**1**) (nia = nicotinamide) or vanillic acid (HL2) $[Cu(L2)_2(nia)_2]$ (**2**) $[Cu_2(\mu\text{-}L2)_4(nia)_2]$ (**3**), and $[Cu(L2)_2(Hetam)_2]$ (**4**) (Hetam = ethanolamine) were isolated and characterized. The molecular structure of complex **1** reveals bidentate vanillin (HL1) coordination *via* the methoxy and the deprotonated hydroxy groups. On the other hand, the vanillic acid (HL2) complexes **2** – **4** show a deprotonated carboxylate group with chelating coordination mode in **2**, bridging in **3** and monodentate coordination in **4**. The mononuclear complexes **1**, **2** and **4** show a distorted *trans* octahedral coordination sphere with pairs of monodentate and chelating ligands. A replacement of the monodentate nicotinamide ligand in **2** with the bidentate ethanolamine ligand in **4** changes the coordination mode of the vanillic acid anion from bidentate (complex **2**) to monodentate (complex **4**). This shift inside the coordination sphere reveals different O–Cu–O Jahn-Teller axes by the vanillic acid anion in **2** and ethanolamine in **4**. Empty channels are present in the crystal structure of the dinuclear complex **3**, stabilized by hydrogen bonds and $\pi$-$\pi$ stacking.

*Key words:* Copper, Guaiacyl, Lignin, Vanillin, Vanillic Acid, *N*-Donor Ligands

## Introduction

Copper-based wood preservatives are widely used due to the significant fungicidal activity of copper and its environmental acceptability [1 – 3]. Presumably, these preservatives will be used for wood preservation also in the following decades as there is no economically acceptable alternative available as yet. The interactions of copper with wood are one of the elements determining its role in the wood protection process. In particular, such a copper formulation has to satisfy several requirements concerning its penetration into wood, a fixation there and prevention of water leaching [4]. All these details are key elements especially for an efficient outdoor wood protection. It was suggested that the main copper-to-wood interaction takes place *via* lignin and hemicellulose [5, 6]. The specific coordination sites of the naturally occurring macromolecular lignin are simulated by different phenyl types of model ligands. Syringyl (4-hydroxy-3,5-dimethoxyphenyl), guaiacyl (4-hydroxy-3-methoxyphenyl) and *p*-hydroxyphenyl derivatives all comprise methoxy and hydroxy oxygen coordination sites (Scheme 1). The softwood lignin is mainly composed of guaiacyl units from the predominant precursor ferulic acid (Scheme 2d) [7]. Beside one cobalt and one nickel complex [8], only copper complexes with vanillin or vanillic acid as ligands (Scheme 2) have been reported for this family in the literature [8 – 17]. All examples reveal deprotonation of vanillin and vanillic acid and their bidentate coordination *via* hydroxy and methoxy groups in the case of vanillin, while vanillic acid coordinates through its carboxylate group. Water is the most convenient solvent for an application of copper-based wood protection formulations, though organic solvents should not be excluded. To prepare a suitable wood protecting formulation, the fixation agent and some other additives are needed next to cooper and

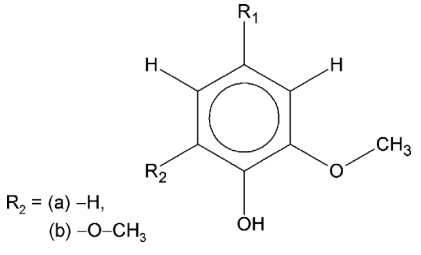


Scheme 1. Two families of lignin model compounds: guaiacyl (a) and syringyl (b).

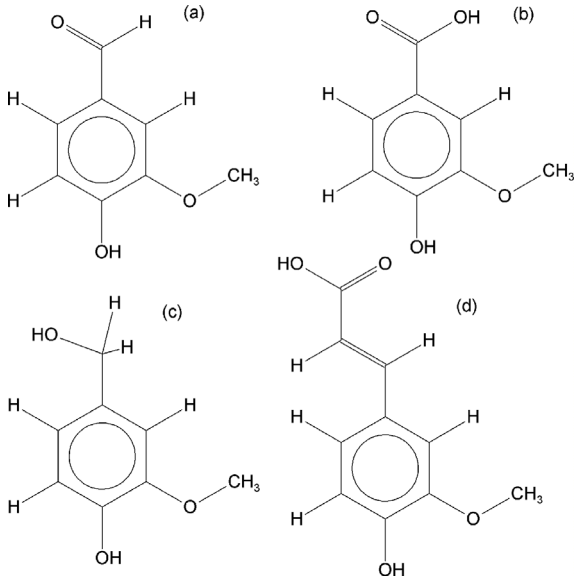


Scheme 2. The guaiacyl lignin model compounds: (a) 4-hydroxy-3-methoxybenzaldehyde (vanillin), (b) 4-hydroxy-3-methoxybenzoic acid (vanillic acid), (c) 4-hydroxy-3-methoxybenzyl alcohol, and (d) 3-(4-hydroxy-3-methoxyphenyl)prop-2-enoic acid (ferulic acid).

the appropriate solvent. During the last two decades, ammonia- and amine-based fixation agents [5, 6, 18] have replaced highly toxic chromium(VI) compounds used in the old formulations [19, 20]. Ethanolamine (Hetam) seems to be the most appropriate replacement for chromium [18, 21]. Copper(II) ions easily form cationic Cu-Hetam species [22] helping the copper penetration into wood, but can be washed out of it as well. Efforts to prevent such leaching are currently in progress [4]. On the other hand, the addition of nicotinamide showed enhanced fungicidal activity of the binuclear fatty acid copper(II) carboxylates [23]. This is important, because copper(II) itself cannot ensure sufficient protection against wood destroying organisms, which is the reason why in practice other cobiocides are combined with copper(II) [24].

Herein, we present four new copper(II) complexes with two lignin model ligands, *viz.* vanillin (HL1) and vanillic acid (HL2): $[Cu(L1)_2(nia)_2]$ **1** (nia = nicotinamide), $[Cu(L2)_2(nia)_2]$ **2**, $[Cu_2(\mu\text{-}L2)_4(nia)_2]$ **3** and $[Cu(L2)_2(Hetam)_2]$ **4** (Hetam = ethanolamine). In addition to the lignin model ligands, the nitrogen donor ligand nicotinamide is additionally coordinated in all cases. The particular combination of both types of ligands is crucial for the coordination mode realized in these complexes.

## Experimental Section

*Synthesis*

$[Cu(L1)_2(H_2O)_2]$ (HL1 = vanillin) was prepared *via trans*-$[Cu(L1)_2(H_2O)_2] \cdot 2H_2O$, which decomposes in air, as described previously [16]. All other chemicals were readily available from commercial sources and were used as received without further purification.

*[Cu(L1)$_2$(nia)$_2$] (**1**)*

Nicotinamide (0.35 g, 2.9 mmol) was dissolved in 20 mL of methanol. This solution was added to solid $[Cu(L1)_2(H_2O)_2]$ (HL1 = vanillin) (0.32 g, 0.80 mmol). After one day, gold-brown crystals of **1** started to precipitate beside undissolved $[Cu(L1)_2(H_2O)_2]$. The solid mixture was stirred with a glass rod, and after 24 h pure **1** was filtered off and dried over KOH for one day. Yield 65 %. – Anal. for $C_{28}H_{26}CuN_4O_8$ (610.1): calcd. C 55.13, H 4.30, N 9.18, Cu 10.42; found C 54.9, H 4.41, N 8.78, Cu 10.80. – IR: $\nu$ = 3355, 3175 (N–H), 1695 $(C{=}O)_{nia}$, 1653 $(C{=}O)_{L1}$, 1582, 1557, 1490, 1470, 1435 ($CH_3$), 1385, 1305 $cm^{-1}$. – UV/Vis: $\lambda_{max}$ = 260, 330, 470(sh) 620 nm. – EPR (298 K): $g_\perp = 2.07$, $g_\parallel = 2.34$, $A_\parallel = 10.9$ mT. – $\chi$ (298 K): $\mu_{eff} = 1.95\ \mu_B$.

*[Cu(L2)$_2$(nia)$_2$] (**2**)*

Vanillic acid (HL2; 0.25 g, 1.5 mmol) was added to a water solution (20 mL) of $Cu(NO_3)_2 \cdot 3H_2O$ (0.19 g, 0.79 mmol). Nicotinamide (1.4 g, 11.5 mmol) was simultaneously dissolved in 20 mL of water and then added to vanillic acid in the copper nitrate solution. Violet crystals of **2** soon started to precipitate. They were filtered off after 2 d and dried over KOH for a day. Yield 65 %. – Anal. for $C_{28}H_{26}CuN_4O_{10}$ (642.1): calcd. C 52.38, H 4.08, H 8.73, Cu 9.90; found C 51.90, H 4.15, N 8.52, Cu 10.20. – IR: $\nu$ = 3385, 3260, 3140 (O–H), (N–H), 1690 $(C{=}O)_{nia}$, 1625, 1604, 1594, 1536 $(O_2C)_{as}$, 1511, 1465, 1440 ($CH_3$), 1394 $(O_2C)_s$, 1354 $cm^{-1}$. – UV/Vis: $\lambda_{max}$ = 220, 270, 290, 400(sh), 510, 560(sh) nm. – EPR (298 K): $g_\perp = 2.06$, $g_\parallel = 2.34$. – $\chi$ (298 K): $\mu_{eff} = 1.93\ \mu_B$.

*[Cu$_2$($\mu$-L2)$_4$(nia)$_2$] (**3**)*

Solid $Cu_2O$ (20 mg, 0.14 mmol), vanillic acid (80 mg, 0.48 mmol) and nicotinamide (80 mg, 0.66 mmol) were homogenized. 20 mL of acetonitrile was added to the solid mixture, and the obtained suspension was stirred and then left standing for 24 h. Green needle-like crystals of **3** were filtered off, washed with acetonitrile, and dried over KOH for 24 h. Yield 35 %. – Anal. for $C_{44}H_{40}Cu_2N_4O_{18}$ (1039.9): calcd. C 50.82, H 3.88, N 5.39, Cu 12.22; found C 50.19, H 3.89, N 5.69, Cu 11.70. – IR: $\nu$ = 3400, 3160 (O–H), (N–H), 1685 $(C{=}O)_{nia}$, 1620, 1600, 1570 $(O_2C)_{as}$, 1515, 1455, 1427 ($CH_3$), 1390 $(O_2C)_s$ $cm^{-1}$. – UV/Vis: $\lambda_{max}$ = 270, 300, 400(sh), 580(sh), 720 nm. – EPR (298 K): $g_\perp$ =

Table 1. Relevant crystal data and data collection summary for **1** – **4**.

| | **1** | **2** | **3** | **4** |
|---|---|---|---|---|
| Formula | $C_{28}H_{26}CuN_4O_8$ | $C_{28}H_{26}CuN_4O_{10}$ | $C_{44}H_{40}Cu_2N_4O_{18}$ | $C_{20}H_{28}CuN_2O_{10}$ |
| Formula weight | 610.08 | 642.08 | 1039.90 | 519.99 |
| Crystal color | brown | violet | green | blue |
| Crystal shape | prism | plate | needle | prism |
| Crystal size, mm$^3$ | $0.40 \times 0.2 \times 0.14$ | $0.40 \times 0.20 \times 0.05$ | $0.55 \times 0.09 \times 0.02$ | $0.12 \times 0.10 \times 0.10$ |
| Crystal system | monoclinic | monoclinic | monoclinic | monoclinic |
| Space group | $C2/c$ | $P2_1/n$ | $P2_1/c$ | $P2_1/n$ |
| $a$, Å | 20.0558(3) | 9.0111(2) | 11.0012(2) | 10.2017(2) |
| $b$, Å | 9.4856(2) | 17.1988(4) | 19.9877(3) | 6.4205(1) |
| $c$, Å | 16.1960(3) | 9.2702(2) | 11.0368(2) | 17.1375(5) |
| $\beta$, deg | 115.5853(8) | 101.6614(12) | 96.1050(10) | 95.701(1) |
| $V$, Å$^3$ | 2779.02(9) | 1407.04(5) | 2413.10(7) | 1116.95(4) |
| $Z$ | 4 | 2 | 2 | 2 |
| $D_x$, g cm$^{-3}$ | 1.458 | 1.515 | 1.434 | 1.546 |
| $\mu$(Mo$K_\alpha$), mm$^{-1}$ | 0.843 | 0.842 | 0.958 | 1.037 |
| $T$, K | 293 | 293 | 293 | 293 |
| $\theta$ max, deg | 27.80 | 27.47 | 25.34 | 27.48 |
| $hkl$ range | $-25/+26$, $-11/+12$, $\pm21$ | $\pm11$, $\pm22$, $\pm12$ | $-12/+13$, $-23/+24$, $\pm13$ | $-12/+13$, $-7/+8$, $\pm22$ |
| Total data | 20664 | 19100 | 29799 | 15443 |
| Independent data | 3280 | 3199 | 4377 | 2559 |
| $R_{int}$ | 0.037 | 0.031 | 0.053 | 0.034 |
| Observed data [$F^2 \geq 2\sigma(F^2)$] | 2813 | 2602 | 3526 | 2123 |
| Refined parameters | 235 | 196 | 307 | 195 |
| $R^a$ (observed) | 0.033 | 0.041 | 0.041 | 0.038 |
| $Rw^b$ | 0.028 | 0.029 | 0.029 | 0.028 |
| $\Delta\rho_{min/max}$, e Å$^{-3}$ | −0.79/0.41 | −1.03/0.66 | −1.07/0.75 | −1.23/0.44 |

[a] $R = \Sigma(||F_o| - |F_c||)/\Sigma|F_o|$; [b] $Rw = \Sigma(w(|F_o| - |F_c|))/\Sigma(w|F_o|)$.

2.06, $g_{\|}$ = 2.35, $D$ = 0.322 cm$^{-1}$, $-2J$ = 238 cm$^{-1}$. – $\chi$ (294 K): $\mu_{eff}$ = 1.43 $\mu_B$.

*[Cu(L2)$_2$(Hetam)$_2$], (**4**)*

Solid CuI (19 mg, 0.10 mmol) and vanillic acid (50 mg, 0.30 mmol) were homogenized, and 30 mL of acetonitrile was added. The reactants were dissolved by stirring, and a drop of ethanolamine (Hetam) was added after 3 min. Blue crystalline aggregates were filtered off and dried over KOH for one day. Yield 70 %. – Anal. for $C_{20}H_{28}CuN_2O_{10}$ (520.0): calcd. C 46.20, H 5.43, N 5.39, Cu 12.22; found C 46.31, H 5.12, N 5.80, Cu 11.90. – UV/Vis: $\lambda_{max}$ = 270, 300, 400(sh), 570 nm. – IR: $\nu$ = 3305, 3245, 3180 (O–H), (N–H), 1596, 1538 $(O_2C)_{as}$, 1505, 1450 $(CH_3)$, 1398, 1376 $(O_2C)_s$ cm$^{-1}$. – EPR (298 K): $g_\perp$ = 2.06, $g_{\|}$ = 2.28. – $\chi$ (294 K): $\mu_{eff}$ = 1.89 $\mu_B$.

The identity of the compounds was confirmed by powder XRD analysis [25].

Single crystals of compounds **1** – **4**, suitable for X-ray analysis, were obtained by the experimental procedures described above, but using lower concentrations of the reactants.

*Physical measurements*

C, H, N analyses were performed with a Perkin-Elmer, Elemental Analyzer 2400 CHN. Metal analysis was carried out electrogravimetrically with Pt electrodes. Infrared spectra were recorded on a Perkin-Elmer Spectrum 100 FT-IR spectrometer, equipped with a Specac Golden Gate Diamond ATR as a sample support. Electronic spectra were recorded as nujol mulls with a Perkin-Elmer UV/Vis/NIR spectrometer Lambda 19. X-Band EPR spectra of the powdered samples were recorded at r. t. using a Bruker ESP-300 spectrometer. The magnetic susceptibility was recorded at r. t. for powdered samples with a Sherwood Scientific MSB-1 balance. Diamagnetic corrections were estimated from Pascal's constants [26]. Powder XRD data were obtained with a Guinier Enraf Nonius camera for **1** and **2** and with a PANalytical X'Pert PRO MPD diffractometer for **3** and **4**, both operating with Cu$K_\alpha$ radiation.

*Crystal structure analysis*

The diffraction data for complexes **1** – **4** were collected on a Nonius Kappa CCD diffractometer with graphite-monochromated Mo$K_\alpha$ radiation. The data were processed using the programs HKL DENZO, SCALEPACK [27]. All four structures were solved by Direct Methods using SIR97 [28] and refined by full-matrix least-squares procedures based on $|F|$ using XTAL3.6 [29]. All non-hydrogen atoms were refined with anisotropic displacement parameters. Most of the positions of the hydrogen atoms (including all hydrogen atoms involved in hydrogen bonding as described in Table 2)

Table 2. Bond lengths (Å), selected angles (deg) and hydrogen bond parameters [distances (Å) and angles (deg)] in **1** – **4**.[a]

| | | | | | | |
|---|---|---|---|---|---|---|
| **1** | Cu–O2 | 2.3925(13) | Cu–O3 | 1.9227(11) | Cu–N1 | 2.0715(13) |
| | O2–Cu–O3 | 76.12(5) | O2–Cu–N1 | 93.69(5) | O3–Cu–N1 | 89.52(5) |
| | O2–Cu–O3$^{i}$ | 103.88(5) | O2–Cu–N1$^{i}$ | 86.31(5) | O3–Cu–N1$^{i}$ | 90.48(5) |
| | D–H···A | D···A | D–H···A | D–H···A | D···A | D–H···A |
| | N2–H22···O1$^{ii}$ | 2.882(3) | 162(3) | N2–H21···O3$^{iii}$ | 2.916(2) | 157(2) |
| **2** | Cu–O1 | 1.9722(11) | Cu–O2 | 2.5884(12) | Cu–N1 | 2.0053(13) |
| | O1–Cu–O2 | 55.95(4) | O1–Cu–N1 | 89.48(5) | O2–Cu–N1 | 87.06(4) |
| | O1–Cu–O2$^{i}$ | 124.05(4) | O2–Cu–N1$^{i}$ | 92.94(4) | O1–Cu–N1$^{i}$ | 90.52(5) |
| | D–H···A | D···A | D–H···A | D–H···A | D···A | D–H···A |
| | O4–H4···O2$^{iv}$ | 2.7329(17) | 153 | N2–H22··· O2$^{v}$ | 3.0386(19) | 162 |
| | O4–H4···O3 | 2.6834(17) | 110 | N2–H21···O5$^{vi}$ | 2.870(2) | 171 |
| **3** | Cu–O1 | 1.9596(17) | Cu–O5 | 1.991(2) | Cu–O2$^{vii}$ | 1.9565(18) |
| | Cu–O6$^{vii}$ | 2.0078(19) | Cu–N1 | 2.159(2) | O1–Cu–O5 | 86.86(9) |
| | O1–Cu–O2$^{vii}$ | 168.92(8) | O1–Cu–O6$^{vii}$ | 88.03(8) | O1–Cu–N1 | 96.60(8) |
| | O5–Cu–O2$^{vii}$ | 90.67(9) | O5–Cu–O6$^{vii}$ | 168.19(8) | O5–Cu–N1 | 96.15(9) |
| | O2$^{vii}$–Cu–O6$^{vii}$ | 92.32(8) | O2$^{vii}$–Cu–N1 | 94.40(8) | O6$^{vii}$–Cu–N1 | 95.00(8) |
| | D–H···A | D···A | D–H···A | D–H···A | D···A | D–H···A |
| | O4–H41···O3 | 2.640(3) | 117 | O8–H8···O7 | 2.701(3) | 136 |
| | O4–H41···O6$^{viii}$ | 2.984(3) | 145 | N2–H201···O9$^{ix}$ | 2.895(4) | 173 |
| **4** | Cu–O1 | 2.0081(9) | Cu–O5 | 2.5697(12) | Cu–N1 | 1.9968(13) |
| | O1–Cu–O5 | 90.21(4) | O1–Cu–N1 | 91.31(5) | O5–Cu–N1 | 75.04(5) |
| | O1–Cu–O5$^{i}$ | 89.79(4) | O1–Cu–N1$^{i}$ | 88.70(5) | O5–Cu–N1$^{i}$ | 104.96(5) |
| | D–H···A | D···A | D–H···A | D–H···A | D···A | D–H···A |
| | O4–H4···O5$^{x}$ | 2.6584(17) | 179(4) | N1–H11···O2$^{xi}$ | 2.9164(16) | 162(3) |
| | O5–H51···O2 | 2.5834(15) | 171(3) | | | |

[a] Symmetry operations: [i] $1-x, 1-y, 1-z$; [ii] $1/2-x, 3/2-y, 1-z$; [iii] $x, 1+y, z$; [iv] $1/2+x, 1/2-y, 1/2+z$; [v] $1-x, 1-y, 2-z$; [vi] $-x, 1-y, 2-z$; [vii] $-x, 1-y, 1-z$; [viii] $x, y, -1+z$; [ix] $1-x, 1-y, -z$; [x] $-1+x, y, z$; [xi] $x, -1+y, z$.

were located using difference Fourier maps. Only the positions of H83 (bonded to C8) in **1**, H2 (bonded to C2) and H14 (bonded to C14) in **3**, and H81 and H83 (both bonded to C8) in **4** were calculated, because those obtained from difference Fourier maps resulted in unacceptable geometries. The parameters of the hydrogen atoms in compounds **2** and **3** were not refined, nor were those of H83 in **1**, and of H81, H82 and H83 in **4**. The positional and isotropic displacement parameters of the remaining hydrogen atoms in **1** and **4** were refined. Crystal data and numbers pertinent to data collection and refinement are listed in Table 1. Selected bond lengths and angles for **1** – **4** are summarized in Table 2. The structure plots were drawn with PLATON [30].

CCDC 671024-671027 contain the supplementary crystallographic data for this paper. These data can be obtained free of charge from The Cambridge Crystallographic Data Centre *via* www.ccdc.cam.ac.uk/data_request/cif.

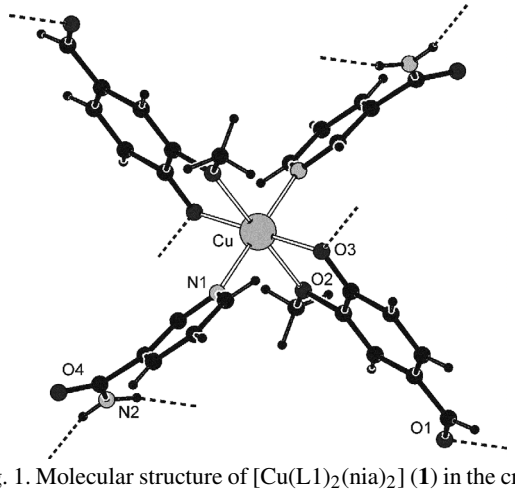


Fig. 1. Molecular structure of $[Cu(L1)_2(nia)_2]$ (**1**) in the crystal showing a typical bidentate vanillin coordination *via* hydroxy and methoxy moieties.

## Results and Discussion

### *Crystal structures*

A centrosymmetric molecule of $[Cu(L1)_2(nia)_2]$ (**1**) (HL1 = vanillin, nia = nicotinamide) is formed by two *trans* oriented nicotinamide molecules and two bidentate vanillin anions (Fig. 1). Nicotinamide is coordinated *via* the ring nitrogen atom [Cu–N1 2.072(2) Å], while vanillin is attached through the deprotonated hydroxyl oxygen atom [Cu–O3 1.923(2) Å] and the methoxy oxygen atom [Cu–O2 2.393(2) Å], the latter forming the elongated Jahn-Teller axis (Table 2). The molecular structure of **1** is similar to

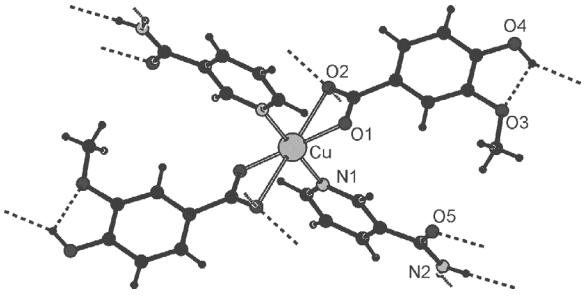


Fig. 2. The molecular structure of $[Cu(L2)_2(nia)_2]$ (**2**) with bidentate chelating carboxylate coordination.

that of other reported vanillin complexes, showing a hydroxy/methoxy bidentate vanillin coordination and an additional ligand in a mononuclear structure [10–14, 16, 17]. Some variation is found in the binuclear vanillin-ethanolamine complex $[Cu_2(\mu\text{-etam})_2(L1)_2]$, where the ethanolamine anion serves as a chelating ligand as well as a monoatomic bridge between the adjacent copper atoms [10]. The nicotinamide amide group in **1** is forming two intermolecular hydrogen bonds to the hydroxy [N2–H21···O3 2.916(2) Å, 157(2)°] and the aldehyde oxygen atoms [N2–H22···O1 2.882(3) Å, 162(3)°]. Apparently, they are the driving force for the crystal packing together with the $\pi$-$\pi$ stacking of the pyridine (nia) rings [centroid···centroid distance 3.860(1) Å, mean inter-planar separation 3.595 Å].

The other lignin model vanillic acid (HL2) in the complexes **2** – **4** is coordinated to the central copper(II) atom by the carboxylate group through three different coordination modes [chelating (**2**), bridging (**3**), and monodentate (**4**), respectively].

The mononuclear complex $[Cu(L2)_2(nia)_2]$ (**2**) is built up by two bidentate vanillic acid anions [Cu–O1 1.972(2) Å, Cu–O2 2.589(2) Å] and two nicotinamide molecules [Cu–N1 2.005(2) Å] in *trans* orientation (Fig. 2). The elongated octahedral coordination sphere $CuO_2N_2O_2$ with a chelating lignin model $L2^-$ is similar as in the vanillin complex **1**, although different coordinating groups are involved, namely carboxylate in **2**, and hydroxy and methoxy oxygen atoms in **1**. This makes an important difference in the hydrogen bonding network due to a hydroxy group acting as hydrogen bond donor in **2** (-O4–H4). It participates in an intramolecular hydrogen bond O4–H4···O3 [2.683(2) Å, 110°] with the methoxy group and in an intermolecular contact O4–H4···O2 [2.733(2) Å, 153°] with a neighboring weakly coordinated carboxylate oxygen atom. Beside them, two nia hydrogen bonds [N2–H21···O5 2.869(2) Å, 171°; N2–H22···O2 3.039(2) Å, 162°] are found, similar as in the structure of **1**. A weak $\pi$-$\pi$ stacking of nia rings [centroid···centroid distance 4.020(1) Å, mean inter-planar separation 3.541 Å] is additionally stabilizing the crystal structure.

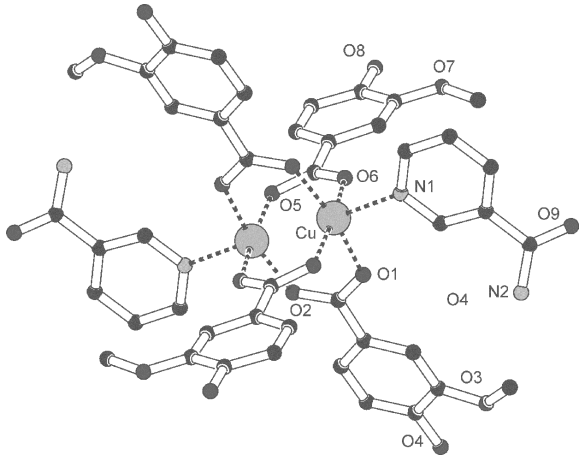


Fig. 3. The dimeric molecular structure of $[Cu_2(\mu\text{-}L2)_4(nia)_2]$ (**3**). Hydrogen atoms are omitted for clarity.

The binuclear complex $[Cu_2(\mu\text{-}L2)_4(nia)_2]$ (**3**) is of the *paddle-wheel* type. Four vanillic acid anions are defining four triatomic carboxylate bridges [Cu–O 1.957(2) – 2.008(2) Å], and two nicotinamide molecules are occupying the apical positions [Cu–N1 2.159(2) Å] of the square-pyramidal $CuO_4N$ coordination geometries *via* their ring nitrogen atoms (Fig. 3). The amide (nia) and the hydroxy (L2) moieties are determining the hydrogen bonding network. Besides the expected intramolecular methoxy/hydroxy hydrogen bonds [O4–H41···O3 2.640(3) Å, 117°; O8–H8···O7 2.701(3) Å, 136°], one of the vanillic acid hydroxy groups is additionally intermolecularly hydrogen-bonded to a carboxylate oxygen atom [O4–H41···O6 2.984(3) Å, 145°]. Each nicotinamide molecule is forming two symmetry-equivalent intermolecular hydrogen bonds with the nicotinamide molecule of the adjacent binuclear unit [N2–H201···O9 2.895(4) Å, 173°]. In addition to extensive hydrogen bonding, efficient $\pi$-$\pi$ stacking [nia pyridine rings centroid···centroid distance 3.555(2) Å, mean inter-planar separation 3.424 Å] stabilizes the structure and leads to empty channels, as can be seen in the crystal structure diagram (Fig. 4). These channels are not destroyed after filtration of the solid compound

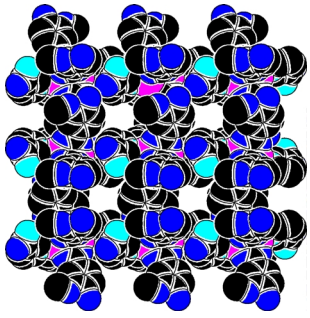

Fig. 4. Empty channels in the crystal structure of $[Cu_2(\mu\text{-}L2)_4(nia)_2]$ (**3**) as shown in the space-filling structure representation. Hydrogen atoms are omitted for clarity.

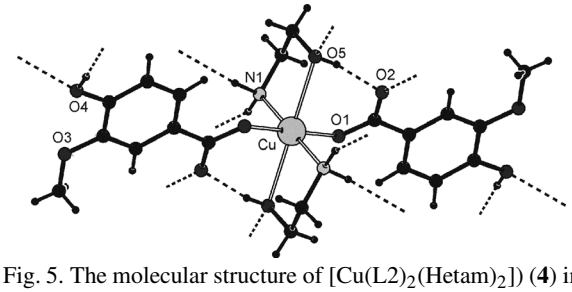


Fig. 5. The molecular structure of $[Cu(L2)_2(Hetam)_2]$) (**4**) in the crystal, showing an extensive inter- and intra molecular hydrogen bonding network.

and thus its separation from the solvent acetonitrile, as was shown by powder diffraction.

Compound $[Cu(L2)_2(Hetam)_2]$ (**4**) (Hetam = ethanolamine) differs from the other three complexes reported herein due to Hetam as a *N*-donor ligand instead of nia which is present in **1** – **3**. Nicotinamide is preferably acting as a monodentate ligand, and only a few examples of a bridging coordination mode have been reported [31 – 33]. On the other hand, in **4** neutral ethanolamine acts as a bidentate ligand *via* the *N*,*O* donor set [Cu–N1 1.997(2) Å, Cu–O5 2.570(2) Å]. This may be the key reason that the vanillic acid carboxylate coordinates *via* one oxygen atom only [Cu–O1 2.008(1) Å] (Fig. 5), and not as a chelate as in the related mononuclear complex **2**. A priority of a chelating coordination of a neutral Hetam ligand over a carboxylate anion within the same complex is noticed also in a related ethanolamine complex [34]. The weak coordination of Hetam *via* the oxygen atom O5, giving the elongated Jahn-Teller axis, is certainly related to the presence of a strong intramolecular hydrogen bond O5–H51···O2 [2.583(2) Å, 171(3)°]. Additionally, both oxygen atoms involved in this hydrogen bond (O5, O2) are also intermolecularly hydrogen-bonded to ethanolamine [N1–H11···O2 2.916(2) Å, 162(3)°] and the hydroxy oxygen atom [O4–H4···O5, 2.658(2) Å, 179(4)°]. The latter hydrogen bond (O4–H4···O5) is crucial for the orientation of the hydrogen atom H4 away from the methoxy oxygen atom O3 of the same vanillic acid anion, which is in contrast to the situation in compounds **2**, **3**, $[Cu_2(\mu\text{-}L2)_4(H_2O)_2]$ [8, 15], and $[Cu_2(\mu\text{-}L2)_2(\mu\text{-}O_2CCH_3)_2(CH_3OH)_2]$ [9], where intramolecular methoxy/hydroxy hydrogen bonds are formed (Table 2). Besides the extensive hydrogen bonding network, $\pi$-$\pi$ stacking is noticeable [centroid···centroid distance 3.574(1) Å, mean interplanar separation 3.419 Å] in **4**. Due to the hydrogen bonding network and the $\pi$-$\pi$ stacking, a competition of two candidates for the bidentate coordination mode, namely L2 and Hetam, results in favor of chelating Hetam and monodentate L2 in **4**, as was discussed above.

*Spectroscopy*

The electronic spectrum of the vanillin complex **1** shows a dominant UV band at 330 nm due to $\pi$-$\pi$ and LMCT transitions, accompanied by a shoulder at 470 nm. In the visible light region, a weak intensity *d*-*d* band at 620 nm appears. The absence of a dominant band in the 600 – 800 nm region and the presence of a stronger intensity shoulder at 400 – 500 nm as observed in the spectrum of the golden-yellow colored compound **1** are also reported for the yellow-green and orange vanillin complexes $[Cu(L1)_2(H_2O)_2]$ [16, 17]. The mononuclear vanillic acid complexes **2** and **4** show a low intensity *d*-*d* band at 500 – 600 nm and a strong 300 nm signal. Both compounds are blue-purple colored as often observed for octahedral Cu(II) complexes. The spectrum of the green binuclear complex **3** shows signals at 270, 300, 400(sh), 580(sh), and 720 nm (*d*-*d*). Compared to the spectra of the mononuclear compounds **1**, **2** and **4**, the spectrum of **3** shows a significantly stronger *d*-*d* band, though not as intensive as in the UV region. The 400(sh) nm band can not be classified as typical for a binuclear complex, since a similar shoulder band appears also in the spectra of mononuclear **1**, **2** and **4**.

IR spectra of the complexes **1** – **4** show signals of the $NH_2$ (nia, Hetam) and OH (L2, Hetam) groups in the region above 3000 $cm^{-1}$. A dominant amide C=O signal at 1690 $cm^{-1}$ is noticed for the nia complexes **1** – **3**, and an additional one for **1** at 1650 $cm^{-1}$ due to vanillin. The signal for the asymmetric stretch-

ing of the carboxylate group (vanillic acid anion) in **3** is found as expected at 1570 $cm^{-1}$, whereas it appears for the mononuclear complexes **2** and **4** at unusually low energy (1540 $cm^{-1}$). Similar low values for $\nu_{as}(O_2C)$ were reported for the related Hetam complex [34] and attributed to strong hydrogen bonds of the carboxylate moiety.

The EPR spectrum of the *paddle-wheel*-type complex **3** shows four spin $S = 1$ signals ($H_{z1}$ 9.3, $H_{x2}$ 44.6, $H_{y2}$ 478, $H_{z2}$ 576 mT), characteristic of antiferromagnetically coupled binuclear Cu(II) species ($-2J$ = 238 $cm^{-1}$), while signals at 300 mT can be assigned to mononuclear impurities with spin $S = 1/2$. A clear splitting of the $H_{\perp 2}$ signal into two separate signals $H_{y2}$ and $H_{z2}$ is due to the non-negligible rhombic symmetry zero-field splitting parameter $E$. The elongated axial symmetry signals ($g_\perp$, $g_\parallel$) are found in the spectra of all three mononuclear species **1**, **2** and **4**. Poorly resolved hyperfine splitting $A_\parallel$ (10.9 mT) is noticed for the complex **1**.

The room temperature magnetic susceptibility measurements give $\mu_{eff}(\mu_B)$ values of 1.95 (**1**), 1.93 (**2**), 1.43 (**3**), and 1.89 (**4**) that are in agreement with the observed EPR spectra and molecular structures for all four complexes **1** – **4**.

## Conclusions

The copper complexes $[Cu(L1)_2(nia)_2]$ (**1**), $[Cu(L2)_2(nia)_2]$ (**2**), $[Cu_2(\mu\text{-}L2)_4(nia)_2]$ (**3**) and $[Cu(L2)_2(Hetam)_2]$) (**4**), with two different types of ligands (the lignin model and the nitrogen donor molecule) show a variety of coordination geometries. Two lignin models, vanillin (L1) and vanillic acid anions (L2), prefer to coordinate as bidentate ligands *via* methoxy/hydroxy (vanillin) or carboxylate (vanillic acid) groups. A large group of the previously reported lignin model complexes reveal an additional nitrogen ligand in the coordination sphere [10 – 14], though oxygen donor ligands may be suitable as well [8, 9, 15 – 17]. In some of the latter complexes, *e. g. cis*-, *trans*-$[Cu(L1)_2(H_2O)_2]$ and $[Cu_2(L2)_4(H_2O)_2]$, water is completing the Cu-lignin model coordination sphere, suggesting easy water binding and thus a disturbance of a copper protected wood by outdoor washing. On the other hand, the presence of a strongly bonded *N*-donor ligand allows versatile coordination possibilities even with relatively small molecules such as nicotinamide and ethanolamine. The formation of the copper-to-lignin model complexes is additionally stabilized by hydrogen bonding and $\pi$-$\pi$ stacking interactions. An application of the suitable ligand may support the copper fixation to the natural lignin, thus improving the copper-based wood-protecting formulations.

*Acknowledgements*

We thank Dr. Miha Humar, Biotechnical Faculty, University of Ljubljana for helpful discussions and Dr. Marjeta Šentjurc, EPR Center, 'Jožef Stefan' Institute, Ljubljana, for the EPR data. The financial support of MVZT L4-6209, P1-0175-103, Republic of Slovenia, is gratefully acknowledged.

[1] M. Connell, in *The Chemistry of Wood Preservation* (Ed.: R. Thompson), The Royal Society of Chemistry, Cambridge **1991**, pp. 16 – 33.
[2] M. M. Gharieb, M. I. Ali, A. A. El-Shoura, *Biodegradation* **2004**, *15*, 49 – 57.
[3] N. Druz, I. Andersone, B. Andersons, *Holzforschung* **2001**, *55*, 13 – 15.
[4] M. Humar, D. Žlindra, F. Pohleven, *Build. Environ.* **2007**, *42*, 578 – 583.
[5] P. A. Cooper, *Wood Fiber Sci.* **1998**, *30*, 382 – 395.
[6] J. Zhang, D. P. Kamden, *Holzforschung* **2000**, *54*, 119 – 122.
[7] A. Sakakibara, in *Wood and Cellulosic Chemistry* (Eds.: D. N.-S. Hon, S. Nobuo), Marcel Dekker, New York **1991**, pp. 113 – 175.
[8] T. Glowiak, H. Kozlowski, L. S. Erre, B. Gulinati, B. G. Micera, A Pozzi, S. Bruni, *J. Coord. Chem.* **1992**, *25*, 75 – 84.
[9] B. Kozlevčar, D. Odlazek, A. Golobič, A. Pevec, P. Strauch, P. Šegedin, *Polyhedron* **2006**, *25*, 1161 – 1166.
[10] J. N. R. Ruddick, C. S. Xie, F. G. Herring, *Holzforschung* **2001**, *55*, 585 – 589.
[11] C. S. Xie, J. N. R. Ruddick, S. J. Rettig, F. G. Herring, *Holzforschung* **1995**, *49*, 483 – 490.
[12] R. J. Hobson, M. F. C. Ladd, D. C. Povey, *J. Cryst. Mol. Struct.* **1973**, *3*, 377 – 388.
[13] T. J. Greenhough, M. F. C. Ladd, *Acta Crystallogr.* **1978**, *B34*, 2619 – 2621.
[14] T. J. Greenhough, M. F. C. Ladd, *Acta Crystallogr.* **1978**, *B34*, 2744 – 2752.
[15] Z. Longguan, S. Kitagawa, H. C. Chang, H. Miyasaka, *Mol. Cryst. Liquid Cryst.* **2000**, *342*, 97 – 102.
[16] B. Kozlevčar, B. Mušič, N. Lah, I. Leban, P. Šegedin, *Acta Chim. Slov.* **2005**, *52*, 40 – 43.

[17] B. Kozlevčar, M. Humar, P. Strauch, I. Leban, *Z. Naturforsch*. **2005**, *B60*, 1273 – 1277.
[18] M. Humar, D. Žlindra, F. Pohleven, *Acta Chim. Slov*. **2007**, *54*, 154 – 159.
[19] A. Pizzi, *Holzforschung* **1993**, *47*, 253 – 260.
[20] F. S. Jorge, T. M. Santos, J. P. de Jesus, W. B. Banks, *Wood Sci. Technol*. **1999**, *33*, 487 – 499.
[21] J. Z. Cao, D. P. Kamdem, *Holzforschung* **2004**, *58*, 32 – 38.
[22] I. A. Cody, S. I. Woodburn, M. W. Blackmore, R. J. Magee, *J. Inorg. Nucl. Chem*. **1970**, *32*, 3263 – 3269.
[23] B. Kozlevčar, N. Lah, I. Leban, I. Turel, P. Šegedin, M. Petrič, F. Pohleven, A. J. P. White, D. J. Williams, G. Giester, *Croat. Chem. Acta* **1999**, *72*, 427 – 441.
[24] M. Humar, D. Žlindra, F. Pohleven, *Holz Roh Werkst*. **2007**, *65*, 17 – 21.
[25] X'PERT HIGHSCORE PLUS, PANalitical B. V., Almelo (The Netherlands) **2005**.
[26] R. L. Dutta, A. Syamal, *Elements of Megnatochemistry*, Affiliated East-West PVT Ltd., New Delhi **1993**, pp. 6 – 11.
[27] Z. Otwinowski, W. Minor, *Methods in Enzymology*, Vol. 276, *Macromolecular Crytallography*, Part A (Eds.: C. W. Carter Jr., R. M. Sweet), Academic Press, New York **1997**, pp. 307 – 326.
[28] A. Altomare, M. C. Burla, M. Camalli, G. Gascarano, C. Giacovazzo, A. Gualiardi, A. G. G. Moliterni, G. Polidori, R. Spagna, SIR97, *J. Appl. Crystallogr*. **1999**, *32*, 115 – 119.
[29] S. R. Hall, D. J. du Boulay, R. Olthof-Hazekamp (Eds.), The XTAL3.6 System, University of Western Australia, Lamb, Perth (Australia) **1999**.
[30] A. L. Spek, PLATON, A Multipurpose Crystallographic Tool, Utrecht University, Utrecht (The Netherlands) **2000**. See also: A. L. Spek, *A. Appl. Cryst*. **2003**, *36*, 7 – 13.
[31] B. Kozlevčar, I. Leban, I. Turel, P. Šegedin, M. Petrič, F. Pohleven, A. J. P. White, D. J. Williams, J. Sieler, *Polyhedron* **1999**, *18*, 755 – 762.
[32] C. Cakir, I. Bulut, K. Aoki, *J. Chem. Crystallogr*. **2003**, *33*, 875 – 884.
[33] D. Valigura, J. Moncol, M. Korabik, Z. Pucekova, T. Lis, J. Mrozinski, M. Melnik, *Eur. J. Inorg. Chem*. **2006**, 3813 – 3817.
[34] M. Petrič, F. Pohleven, I. Turel, P. Šegedin, A. J. P. White, D. J. Williams, *Polyhedron* **1998**, *17*, 255 – 260.